Electronic Supplementary Material (ESI) for Environmental Science: Water Research & Technology.

Supporting Information for:

Effects of operating and design parameters on ion exchange columns for nutrient recovery from urine

William A. Tarpeh[†#], Ileana Wald[†#], Maja Wiprächtiger[‡], and Kara L. Nelson[†#*]

[†]Department of Civil and Environmental Engineering, University of California, Berkeley, CA 94720, United States
[#]Engineering Research Center for Re-inventing the Nation's Urban Water Infrastructure (ReNUWIt), United States
[‡]Institute of Environmental Engineering, ETH Zürich, Stefano-Franscini-Platz 5, CH-8093 Zürich, Switzerland

17 pages
9 equations
11 tables
12 figures

*Corresponding author: karanelson@berkeley.edu

S1. EQUATIONS

S1.1 Adsorption and Regeneration in Columns

Breakthrough curves and elution curves were generated from continuous adsorption and regeneration experiments, respectively. Integration of both curves allowed for calculation of the mass of ammonium adsorbed or eluted. Numerical integration was performed using the trapezoid rule:

$$\int C(BV)dBV \approx \sum_{1}^{n}\{(BV_n - BV_{n-1}) * \frac{1}{2} * [C(BV_n) + C(BV_{n-1})]\} \quad \text{(S1)}$$

Where n is the number of data points, BV is number of bed volumes, and C(BV) is the concentration at a given number (BV) of bed volumes. For adsorption experiments, the mass of ammonium adsorbed was proportional to the area above the ammonium breakthrough curve and below the chloride tracer curve. For regeneration, the mass of ammonium eluted is proportional to the area below the elution curve. The equations for recovery efficiency (Equation S2) and adsorption density (Equation S3) are:

$$q = \frac{\int [C_{Cl,ads}(BV) - C_{N,ads}(BV)]dBV * PV}{W * MW_N} \quad \text{(S2)}$$

$$\eta_{regen} = \frac{\int C_{N,elution}(BV)dBV}{\int [C_{Cl,ads}(BV) - C_{N,ads}(BV)]dBV} \quad \text{(S3)}$$

Where PV is pore volume (L bed volume^{-1}), the volume of liquid retained by a column full of resin, W is resin mass (g resin), q is adsorption density (mmol N g resin^{-1}), MW_N is the molar mass of nitrogen (14 g N mol N^{-1}), and the subscripts on concentration C(BV) denote adsorption

or elution. Pore volume was calculated by subtracting the mass of a column full of dry resin from the same column filled with resin and distilled water.

The number of bed volumes to 90% elution was calculated via interpolation of elution curve data points and cumulative area under the elution curve compared to total area (Equation S4):

$$BV_{90} = BV\Big|_{\frac{\int_0^x C_{N,elution}(BV)dBV}{\int_0^f C_{N,elution}(BV)dBV} = 0.9} \quad \text{(S4)}$$

Where x denotes cumulative bed volumes and f denotes the final bed volumes (end of experiment). Thus, bed volumes to 90% elution was calculated as the number of bed volumes at which 90% of the total mass eluted was reached, regardless of overall recovery efficiency.

S1.2 Predicting phosphate adsorption density

Phosphate adsorption density was predicted based on a Freundlich model of best fit determined from batch experiments in real hydrolyzed urine (Equation S5):[1]

$$q_e = K_f C_e^{1/n} \quad \text{(S5)}$$

Where q_e is equilibrium adsorption density (mg P g resin^{-1}), C_e is equilibrium phosphate concentration (mg P L^{-1}), and K_f (mg$^{1-1/n}$ L$^{1/n}$ g^{-1}) and 1/n (unitless) are Freundlich constants. The Freundlich model was combined with a mass balance (Equation S6) to predict equilibrium adsorption density.

$$\frac{W}{V}(q_e - q_0) = C_0 - C_e \quad \text{(S6)}$$

In Equation S6, W/V is resin dose (g resin L^{-1}), q is adsorption density (mg P g $resin^{-1}$), C is aqueous phosphate concentration (mg P L^{-1}), and subscripts denote equilibrium (e) and initial (0) conditions.

Equations S5 and S6 were combined to predict adsorption density assuming no initial P on the resin (q_0=0), a resin dose of 10.036 g L^{-1},[1] Freundlich best-fit parameters from Sendrowski and Boyer 2013 (n=0.353, K_f=0.999),[1] and an initial phosphate concentration of 430 g P^{-1} (measured in this study). The predicted value for q_e was 0.255 mmol P g $resin^{-1}$, which was reported in section 3.1.1 of the main manuscript.

S1.3 Up-concentration in ammonium sulfate product

Concentrations of ammonium sulfate fertilizer product were calculated by determining the maximum of the quotient of the area under the elution curve and elution time using Equation S7 (results in Table S10).

$$C_{product} = Max\left\{\frac{\int C_{N,elution}(BV)dBV}{BV}\right\} \quad \text{(S7)}$$

Available liquid ammonium sulfate is most often 8-9% N,[2,3] which is 80.7-89.6 g N L^{-1} as calculated in Equation S8.

$$\frac{8\ g\ N}{100\ g\ AS\ solution} * \frac{100\ g\ AS}{21\ g\ N} * \frac{1\ g\ solution}{mL\ solution} * \frac{1000\ mL\ solution}{1\ L\ solution} * \frac{1\ mol\ AS}{132.14\ g\ AS} * \frac{2\ mol\ N}{1\ mol\ AS} * \frac{14\ g\ N}{1\ mol\ N} = 80.7\ g\ N\ L^{-1} \quad \text{(S8)}$$

Where AS is ammonium sulfate, which is 21% N by mass(molecular formula $(NH_4)_2SO_4$).

The number of bed volumes required for up-concentration (BV_U) was calculated according to Equation S9:

$$BV_U = \frac{q * W * MW_N}{C_{urine} * P} \quad \text{(S9)}$$

where q is adsorption density (mmol N g resin^{-1}), W is resin mass (g resin), MW_N is the molar mass of nitrogen (mg N mmol N^{-1}), C_{urine} is the total ammonia concentration in urine (mg N L^{-1}), and P is the pore volume (mL bed volume^{-1}). Based on several experimental runs, the resin mass was estimated at 50 g, C_{urine} at 5000 mg N L^{-1}, and adsorption density at 4.9 mmol N g resin^{-1}, giving an estimate of 8 bed volumes.

S2. TABLES

Table S1: Adsorbent characteristics.

Adsorbent	Particle size (mm)	Pore structure[a]	Functional Group	Operating pH	Highest Reported Adsorption Density (mmol N/g. mmol P/g)
Dowex Mac 3	0.3-1.2[4]	Macroporous[4]	Carboxylate	5[4]	4.9[4]
LayneRT	0.3-1.2	Macroporous	Hydrous Iron Oxide	5.5-8.5	0.31[1]

[a]The cut-off between macropores and micropores is 2 nm.[5]

Table S2: Composition of synthetic and real urine. Synthetic urine parameters based on recipe; real urine measured from samples used in these experiments.

	Synthetic Urine	**Real Urine**
pH	8.87	8.99
Total Ammonia Nitrogen (mg N L^{-1})	7950	3820
Sodium (mg Na L^{-1})	2560	1620
Potassium (mg Na L^{-1})	2200	1470
Chloride (mg Cl L^{-1})	4180	3060
Total Phosphate (mg P L^{-1})	542	169
Total Sulfate (mg SO_4 L^{-1})	472	1680
Total Inorganic Carbon (mg C L^{-1})	3250	1860
COD (mg O_2 L^{-1})	8000	3460

Table S3: Synthetic Urine Recipe in 1 L nanopure water. Assumes urea completely hydrolyzed, struvite and hydroxyapatite precipitated, no volatilization, and no citrate/oxalate complexation. [6]

Substance	Amount	
	[g]	[ml]
Na_2SO_4 anhydrous	2.30	
NaH_2PO_4 anhydrous	2.10	
NaCl	3.60	
KCl	4.20	
NH4Ac	9.60	
NH_4OH solution (25% NH_3)		13.0
NH_4HCO_3	21.40	

Table S4. Stock regenerant concentrations from Alibaba.com (accessed May 11, 2016). For NaCl, a saturated solution was assumed based on the solubility of NaCl at 25° C (359 g NaCl L^{-1}).[7]

Regenerant	**C_{stock} (M)**
H_2SO_4	18.21
HCl	10.35
HNO_3	15.47
NaCl	6.143

Table S5: Properties of trace organic contaminants

Abbrev.	Compound	Structure	Function	MW (g/mol)	pKa	Log K_{ow}	Predominant Charge at pH 9
SMX	Sulfamethoxazole	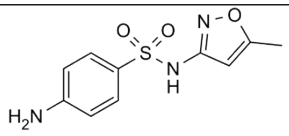	Antibiotic	253.28	1.7, 5.6	0.89[8]	Negative
TMP	Trimethoprim	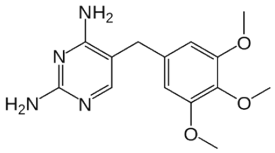	Antibiotic	290.32	7.4	0.79[8]	Positive
ACY	Acyclovir	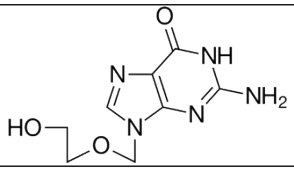	Antiviral	225.21	2.3,9.3	-1.76[8]	Neutral
ZDV	Zidovudine	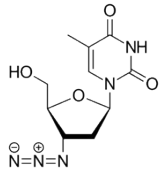	Antiretroviral	267.24	9.7	-0.53[8]	Neutral
ABA	Abacavir	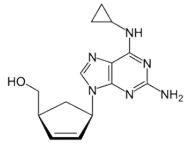	Antiretroviral	286.33	5.01	0.72[8]	Positive
ATE	Atenolol	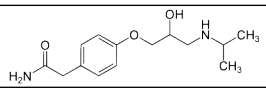	Beta blocker	266.34	9.6	0.16[9]	Positive
MET	Metoprolol	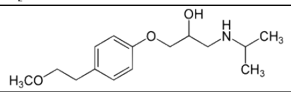	Beta blocker	267.37	9.5	1.76[10]	Positive
CBZ	Carbamazepine	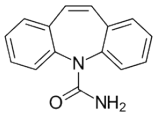	Antiepileptic	236.27	13.9	2.67[10]	Positive
FTC	Emitricitabine	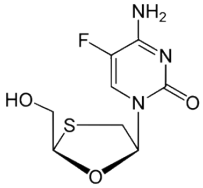	Antiretroviral	247.25	14.3	-3.96[10]	Neutral
ACE	Acetaminophen	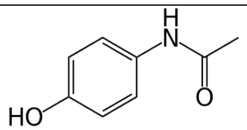	Pain reliever	151.16	9.7	0.34[8]	Neutral

[a]Deborde et al 2008[11] (pH 7)
[b]Barazesh et al 2016[12] (pH 8)

Table S6. Bed volumes to 50% breakthrough, breakthrough curve slopes, and adsorption density for phosphate adsorption in real urine. * denotes significant difference between two rows.

	Bed volumes to 50% breakthrough	Slope (BV^{-1})	Adsorption density (mmol P g $resin^{-1}$)
In series	10.6 ± 0.21	1.13 ± 0.20*	0.50 ± 0.04
Mixed bed	7.70 ± 0.23	0.69 ± 0.08*	0.53 ± 0.04

Table S7. Bed volumes to 50% breakthrough, breakthrough curve slopes, and adsorption density for ammonium adsorption in real urine. * denotes significant difference between two rows.

	Bed volumes to 50% breakthrough	Slope (BV^{-1})	Adsorption density (mmol N g $resin^{-1}$)
In series	16.1 ± 0.6	0.20 ± 0.05	5.44 ± 0.91
Mixed bed	18.3 ± 0.5	0.19 ± 0.02	6.76 ± 0.50*
Struvite supernatant	18.4 ± 0.8	0.34 ± 0.06	2.54 ± 0.57*
Cation exchange only	14.7 ± 1.4	0.26 ± 0.04	4.10 ± 0.17

Table S8. Bed volumes to 50% breakthrough, breakthrough curve slopes, and adsorption density for potassium adsorption in real urine. * denotes significant difference between two rows.

	Bed volumes to 50% breakthrough	Slope (BV^{-1})	Adsorption density (mmol K g $resin^{-1}$)
In series	8.3 ± 3.9	0.16 ± 0.05	0.32 ± 0.06
Mixed bed	10.7 ± 0.1	0.14 ± 0.03*	0.27 ± 0.02
Struvite supernatant	9.5 ± 5.8	0.31 ± 0.15	0.39 ± 0.16
Cation exchange only	10.7 ± 3.4	0.36 ± 0.02*	0.37 ± 0.06

Table S9. Henry's law constant for selected gases (M atm^{-1}).

Compound	**K_H (M atm^{-1})**
N_2	6.3×10^{-4}
NO	1.9×10^{-3}
N_2O	2.5×10^{-2}
O_2	1.3×10^{-3}
CO_2	3.4×10^{-2}
NH_3	59

Table S10. Ammonium recovery efficiencies, stoichiometric efficiencies, final eluent concentrations, and bed volumes to 90% elution for elution experiments at high concentration and 4.5 mL min^{-1}. Resin was exhausted during adsorption with synthetic urine. TAN is total ammonia nitrogen.

H_2SO_4 Concentration (M)	Bed volumes to 90% elution	Stoichiometric Efficiency (%)	Recovery Efficiency (%)	Final Eluent TAN (g N L^{-1})
0.5	7.52	74.8	93.8	9.13
1	4.62	58.9	100.0	12.0
3	2.93	32.2	87.4	21.7
6	3.28	13.4	91.3	17.2

Table S11. Potassium recovery efficiencies, stoichiometric efficiencies, and bed volumes to 90% elution for triplicate elution experiments with various regenerants. Resin was exhausted during adsorption with synthetic urine. Recovery efficiencies greater than 100% are due to variability of measuring low K concentrations in eluent.

	Bed volumes to 90% elution	Stoichiometric Efficiency (%)	Recovery Efficiency (%)
HNO_3	18.2 ± 1.8	7.2 ± 0.7	134 ± 7.3
HCl	25.4 ± 5.0	6.2 ± 1.2	136 ± 6.7
NaCl	17.3 ± 1.3	8.2 ± 0.7	87.6 ± 9.5
H_2SO_4	16.6 ± 0.9	8.0 ± 0.8	111 ± 1.8

S3. FIGURES

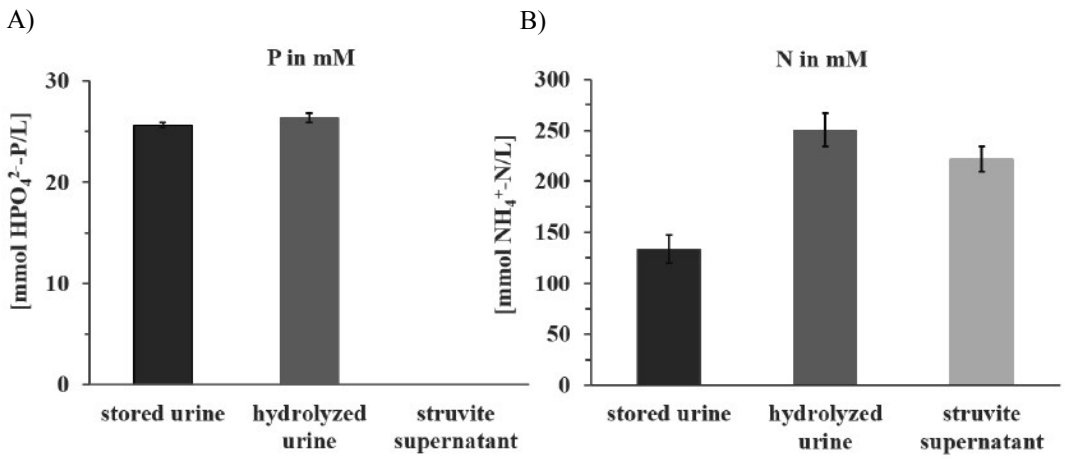

Figure S1. Phosphorus (P) and total ammonia nitrogen (N) concentrations for stored urine, hydrolyzed urine after urease addition, and struvite supernatant (after $MgCl_2$ addition, mixing, and settling). Error bars represent ± one standard deviation for experimental triplicates.

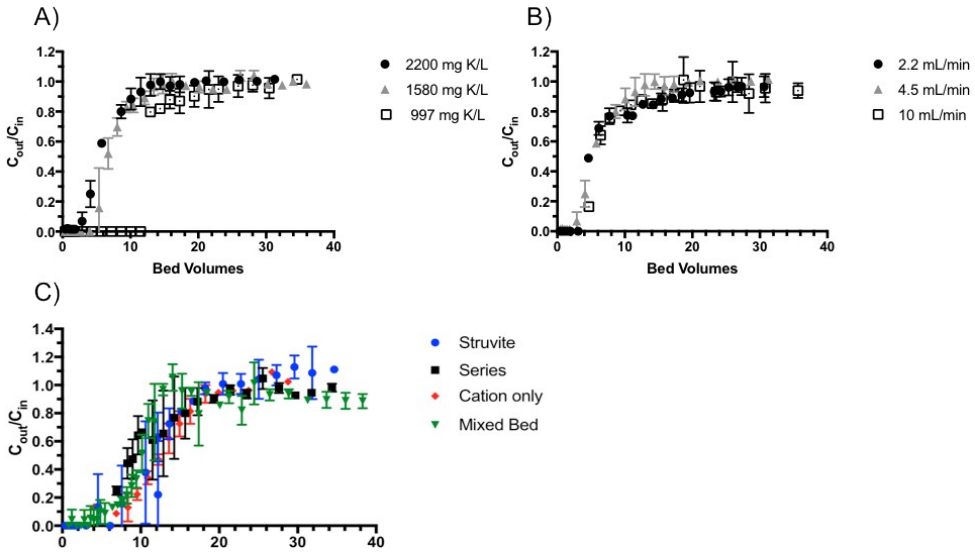

Figure S2. Potassium breakthrough curves with synthetic urine influent for (a) varying influent concentrations (b) varying flow rate and (c) varying setups. Error bars represent ± one standard deviation for experimental triplicates. Error bars not shown are smaller than symbol.

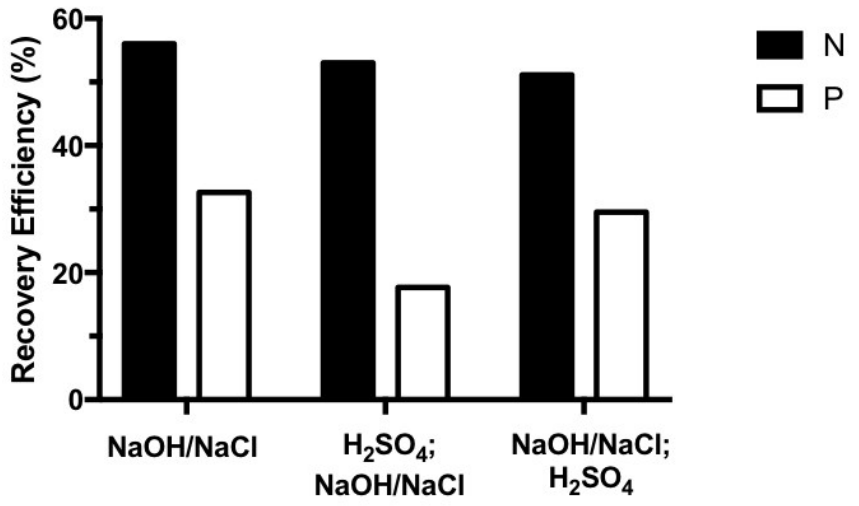

Figure S3. Recovery efficiencies for nitrogen and phosphorus from mixed bed column. Regenerants used were 0.122 M H_2SO_4 and 2% NaOH/ 2% NaCl (0.5 M NaOH/0.342 M NaCl). Semicolon denotes switching regenerants halfway through regeneration experiment (150 min of each solution).

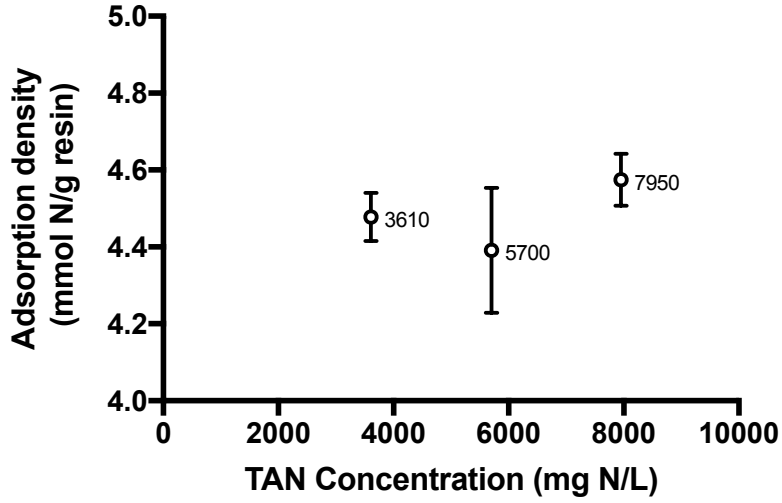

Figure S4. Ammonium adsorption densities vs. concentration for adsorption with synthetic urine at 4.5 mL min^{-1}. Error bars are ± 1 standard deviation. Point labels are TAN concentrations.

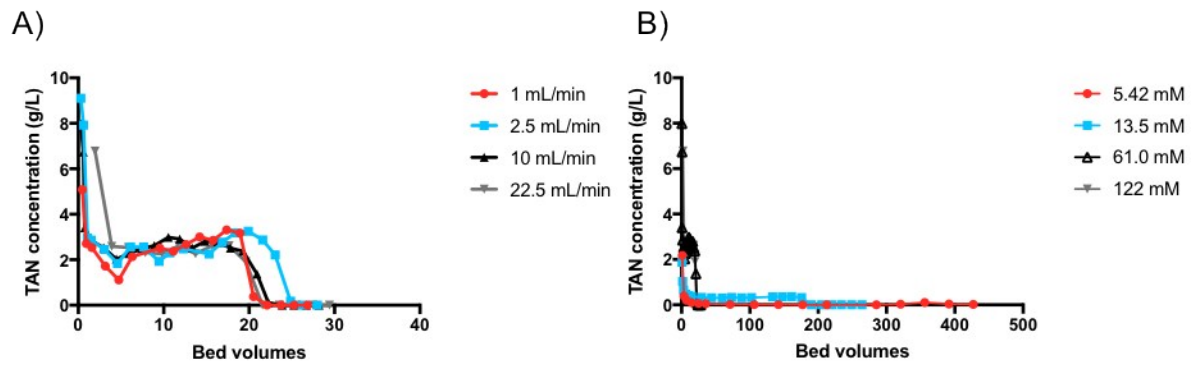

Figure S5. Elution curves for varying (a) flow rate and (b) acid concentration. Flow rate experiments conducted with 0.122 M H_2SO_4 and concentration experiments conducted at 22.5 mL min^{-1}.

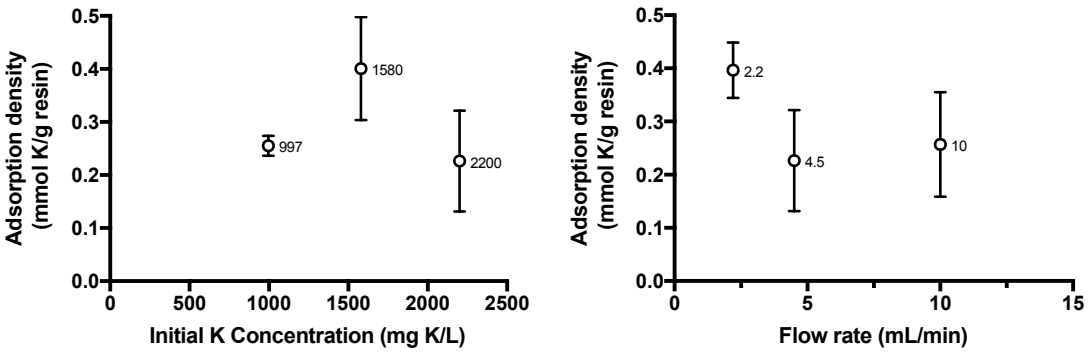

Figure S6. Potassium adsorption densities for varying (a) concentration and (b) flow rate with synthetic urine. Error bars are ± 1 standard deviation.

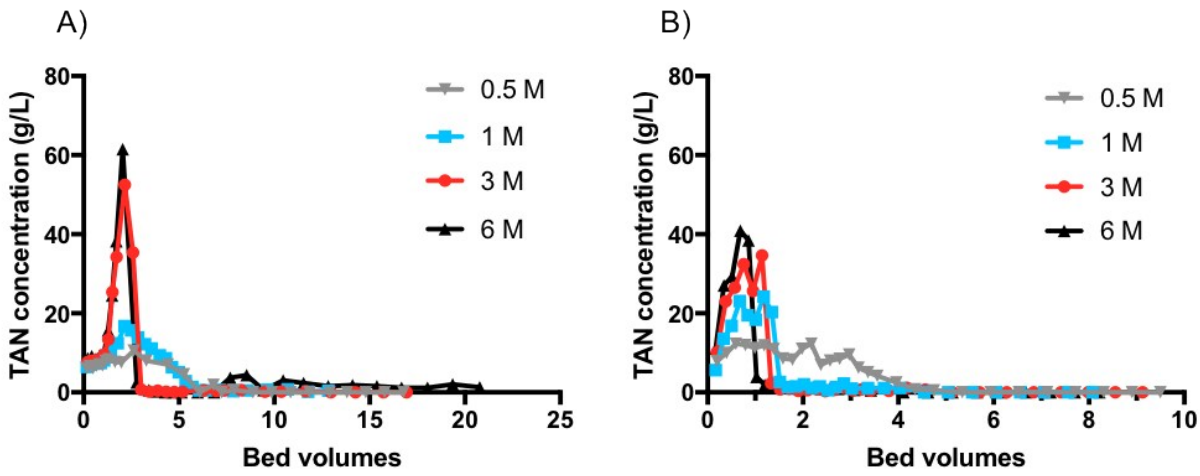

Figure S7. Sulfuric acid elution curves at varying concentrations with (a) 2 mL min^{-1} and (b) 4.5 mL min^{-1} flow rate. Bed volumes to elution, stoichiometric efficiencies, and recovery efficiencies in Table S10 (4.5 mL min^{-1}) and Table 1 (2 mL min^{-1}).

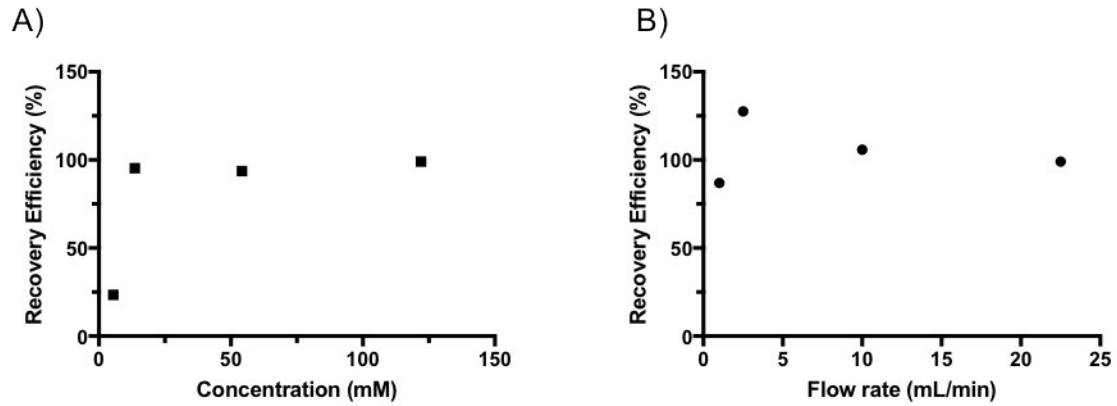

Figure S8. Nitrogen recovery efficiency during elution for varying (a) concentration and (b) flow rate was consistently above 90% for all flow rates tested (1-22.5 mL min^{-1}) and for influent sulfuric acid concentrations greater than or equal to 13.6 mM.

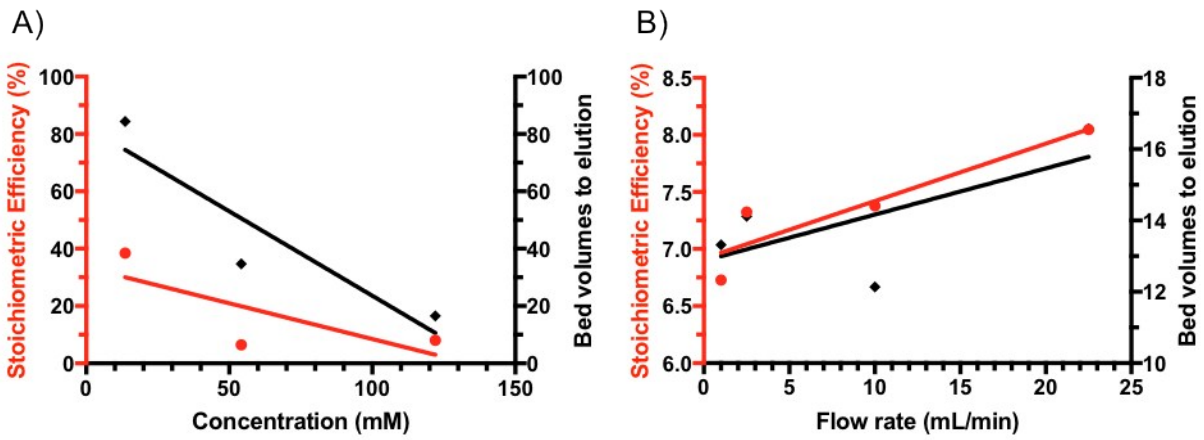

Figure S9. Sulfuric acid use efficiency compared to stoichiometric exchange for potassium elution and column regeneration with (a) varying concentration and (b) varying flow rate. Linear regression lines show slope of each correlation. Resin was exhausted during adsorption with synthetic urine. Lowest concentration excluded because potassium concentrations were below detection limit.

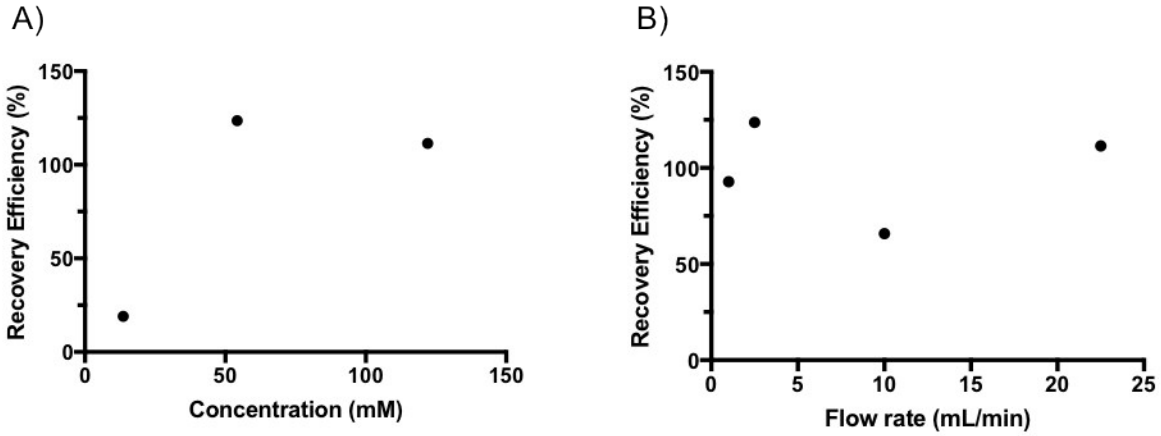

Figure S10. Potassium recovery efficiency for (a) varying regenerant concentration and (b) varying elution flow rate.

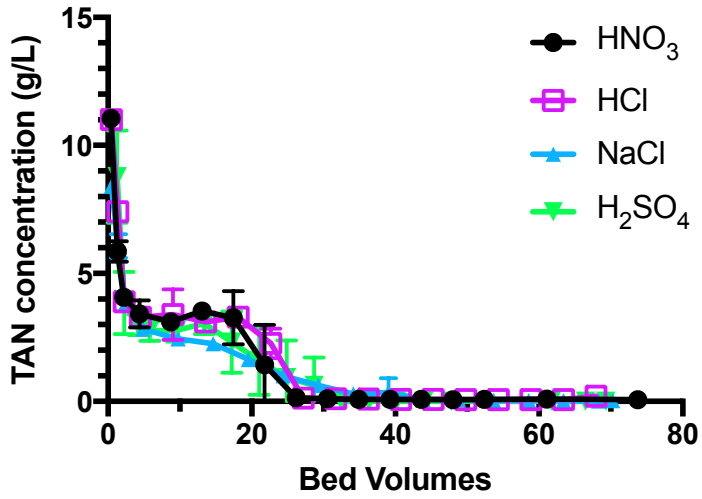

Figure S11. Elution curves for equinormal (0.244 N) regenerants. Error bars are ± 1 standard deviation; some error bars too small to see.

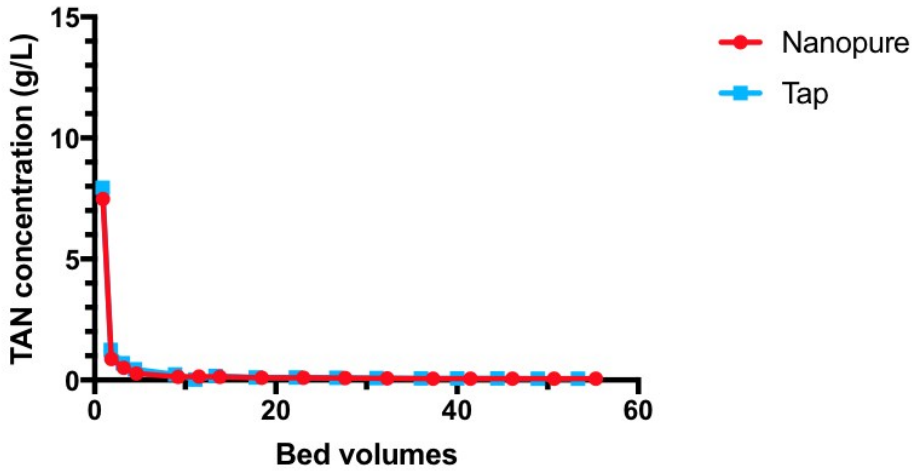

Figure S12. Elution curves for nanopure and tap water. Concentration decreases immediately as synthetic urine elutes from column.

REFERENCES

1 A. Sendrowski and T. H. Boyer, *Desalination*, 2013, **322**, 104–112.
2 O. L. Vargas and D. R. Bryla, *HortScience*, 2015, **50**, 479–485.
3 *Liquid Fertilizer Formulation Guide*, AdvanSix Inc., 2016.
4 *DOWEX MAC-3 Engineering Information*, Dow Chemical Company, Dow Liquid Separations, Midland, MI, 2003.
5 Y. S. Ok, S. M. Uchimiya, S. X. Chang and N. Bolan, *Biochar: Production, Characterization, and Applications*, CRC Press, 2015.
6 K. Udert, T. Larsen and W. Gujer, *Water Sci. Technol.*, 2006, **54**, 413–420.
7 W. M. Haynes, Ed., *CRC Handbook of Chemistry and Physics, 97th Edition*, CRC Press, 97 edition., 2016.
8 R. Shawahna and N. Rahman, *DARU J. Fac. Pharm. Tehran Univ. Med. Sci.*, 2011, **19**, 83–99.
9 M. Mohsen-Nia, A. H. Ebrahimabadi and B. Niknahad, *J. Chem. Thermodyn.*, 2012, **54**, 393–397.
10 B. G. Giménez, M. S. Santos, M. Ferrarini, J. P. S. Fernandes and J. P. S. Fernandes, *Pharm. - Int. J. Pharm. Sci.*, 2010, **65**, 148–152.
11 M. Deborde and U. von Gunten, *Water Res.*, 2008, **42**, 13–51.
12 J. M. Barazesh, C. Prasse and D. L. Sedlak, *Environ. Sci. Technol.*, 2016, **50**, 10143–10152.